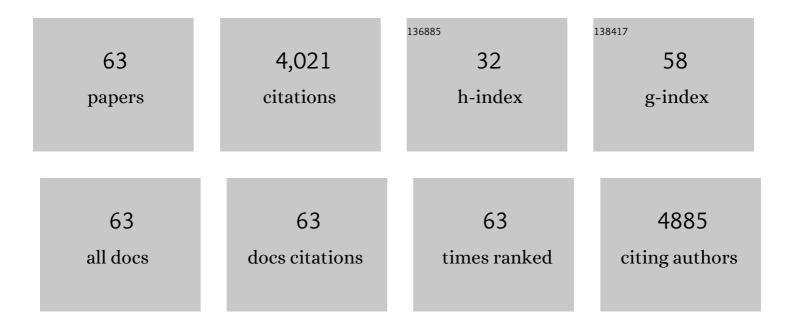
## Michael E Mcconney

List of Publications by Year in descending order

Source: https://exaly.com/author-pdf/5386751/publications.pdf Version: 2024-02-01



#	Article	IF	CITATIONS
1	Voxelated liquid crystal elastomers. Science, 2015, 347, 982-984.	6.0	863
2	Acoustically actuated ultra-compact NEMS magnetoelectric antennas. Nature Communications, 2017, 8, 296.	5.8	299
3	Dynamic color in stimuli-responsive cholesteric liquid crystals. Journal of Materials Chemistry, 2010, 20, 9832.	6.7	276
4	Probing Soft Matter with the Atomic Force Microscopies: Imaging and Force Spectroscopy. Polymer Reviews, 2010, 50, 235-286.	5.3	215
5	Topography from Topology: Photoinduced Surface Features Generated in Liquid Crystal Polymer Networks. Advanced Materials, 2013, 25, 5880-5885.	11.1	194
6	Continuous ultra-thin MoS2 films grown by low-temperature physical vapor deposition. Applied Physics Letters, 2014, 104, .	1.5	178
7	Biologically inspired design of hydrogel-capped hair sensors for enhanced underwater flow detection. Soft Matter, 2009, 5, 292-295.	1.2	114
8	Color-Tunable Mirrors Based on Electrically Regulated Bandwidth Broadening in Polymer-Stabilized Cholesteric Liquid Crystals. ACS Photonics, 2014, 1, 1033-1041.	3.2	101
9	Bioinspired Material Approaches to Sensing. Advanced Functional Materials, 2009, 19, 2527-2544.	7.8	93
10	Contactless, photoinitiated snap-through in azobenzene-functionalized polymers. Proceedings of the National Academy of Sciences of the United States of America, 2013, 110, 18792-18797.	3.3	92
11	Amorphous Boron Nitride: A Universal, Ultrathin Dielectric For 2D Nanoelectronics. Advanced Functional Materials, 2016, 26, 2640-2647.	7.8	90
12	Polymeric Nanolayers as Actuators for Ultrasensitive Thermal Bimorphs. Nano Letters, 2006, 6, 730-734.	4.5	88
13	Thermally Induced, Multicolored Hyperâ€Reflective Cholesteric Liquid Crystals. Advanced Materials, 2011, 23, 1453-1457.	11.1	84
14	Coexistence of Low Damping and Strong Magnetoelastic Coupling in Epitaxial Spinel Ferrite Thin Films. Advanced Materials, 2017, 29, 1701130.	11.1	71
15	Thermo-Optical Arrays of Flexible Nanoscale Nanomembranes Freely Suspended over Microfabricated Cavities as IR Microimagers. Chemistry of Materials, 2006, 18, 2632-2634.	3.2	66
16	Photoinduced hyper-reflective cholesteric liquid crystals enabled via surface initiated photopolymerization. Chemical Communications, 2011, 47, 505-507.	2.2	64
17	Electrically Induced Color Changes in Polymer‣tabilized Cholesteric Liquid Crystals. Advanced Optical Materials, 2013, 1, 417-421.	3.6	63
18	Bandwidth broadening induced by ionic interactions in polymer stabilized cholesteric liquid crystals. Optical Materials Express, 2014, 4, 1465.	1.6	63

MICHAEL E MCCONNEY

#	Article	IF	CITATIONS
19	Viscoelastic nanoscale properties of cuticle contribute to the high-pass properties of spider vibration receptor ( Cupiennius salei Keys). Journal of the Royal Society Interface, 2007, 4, 1135-1143.	1.5	53
20	Characterization of magnetomechanical properties in FeGaB thin films. Applied Physics Letters, 2018, 113, .	1.5	53
21	Optimal Bandgap in a 2D Ruddlesden–Popper Perovskite Chalcogenide for Single-Junction Solar Cells. Chemistry of Materials, 2018, 30, 4882-4886.	3.2	49
22	Surface force spectroscopic point load measurements and viscoelastic modelling of the micromechanical properties of air flow sensitive hairs of a spider ( <i>Cupiennius salei</i> ). Journal of the Royal Society Interface, 2009, 6, 681-694.	1.5	44
23	Direct synthesis of ultra-thin large area transition metal dichalcogenides and their heterostructures on stretchable polymer surfaces. Journal of Materials Research, 2016, 31, 967-974.	1.2	44
24	Photonic crystallization of two-dimensional MoS <sub>2</sub> for stretchable photodetectors. Nanoscale, 2019, 11, 13260-13268.	2.8	43
25	Advances in Transparent Planar Optics: Enabling Large Aperture, Ultrathin Lenses. Advanced Optical Materials, 2021, 9, 2001692.	3.6	43
26	Continuous wave mirrorless lasing in cholesteric liquid crystals with a pitch gradient across the cell gap. Optics Letters, 2012, 37, 2904.	1.7	42
27	Dynamic high contrast reflective coloration from responsive polymer/cholesteric liquid crystal architectures. Soft Matter, 2012, 8, 318-323.	1.2	38
28	Spontaneous Selfâ€Folding in Confined Ultrathin Polymer Gels. Advanced Materials, 2010, 22, 1263-1268.	11.1	37
29	Swelling-Induced Folding in Confined Nanoscale Responsive Polymer Gels. ACS Nano, 2010, 4, 2327-2337.	7.3	37
30	Crystal growth and structural analysis of perovskite chalcogenide BaZrS <sub>3</sub> and Ruddlesden–Popper phase Ba <sub>3</sub> Zr <sub>2</sub> S <sub>7</sub> . Journal of Materials Research, 2019, 34, 3819-3826.	1.2	36
31	Hydrogel microstructures combined with electrospun fibers and photopatterning for shape and modulus control. Polymer, 2008, 49, 5284-5293.	1.8	34
32	Photoresponsive Structural Color in Liquid Crystalline Materials. Advanced Optical Materials, 2019, 7, 1900429.	3.6	34
33	A Facile Fabrication Strategy for Patterning Protein Chain Conformation in Silk Materials. Advanced Materials, 2010, 22, 115-119.	11.1	33
34	Nanorod decorated nanowires as highly efficient SERS-active hybrids. Journal of Materials Chemistry, 2011, 21, 15218.	6.7	32
35	Spin-orbit torque and spin pumping in YIC/Pt with interfacial insertion layers. Applied Physics Letters, 2018, 112, .	1.5	28
36	Integrated magnetoelectric devices: Filters, pico-Tesla magnetometers, and ultracompact acoustic antennas. MRS Bulletin, 2018, 43, 841-847.	1.7	28

3

MICHAEL E MCCONNEY

#	Article	IF	CITATIONS
37	Facile Plasmaâ€Enhanced Deposition of Ultrathin Crosslinked Amino Acid Films for Conformal Biometallization. Small, 2009, 5, 741-749.	5.2	26
38	Electrically Induced Splitting of the Selective Reflection in Polymer Stabilized Cholesteric Liquid Crystals. Advanced Optical Materials, 2020, 8, 2000914.	3.6	23
39	Large-area ultrathin Te films with substrate-tunable orientation. Nanoscale, 2020, 12, 12613-12622.	2.8	22
40	Integrated Tunable Magnetoelectric RF Inductors. IEEE Transactions on Microwave Theory and Techniques, 2020, 68, 951-963.	2.9	20
41	Metalized Porous Interference Lithographic Microstructures via Biofunctionalization. Advanced Materials, 2010, 22, 1369-1373.	11.1	17
42	Electrical Control of Unpolarized Reflectivity in Polymerâ€ <b>5</b> tabilized Cholesteric Liquid Crystals at Oblique Incidence. Advanced Optical Materials, 2018, 6, 1800957.	3.6	17
43	Optically detected ferromagnetic resonance in diverse ferromagnets via nitrogen vacancy centers in diamond. Journal of Applied Physics, 2019, 126, .	1.1	17
44	Role of Alicyclic Conformation-Isomerization in the Photomechanical Performance of Azobenzene-Functionalized Cross-Linked Polyimides Containing Tetra-Substituted Cyclohexane Moieties. ACS Macro Letters, 2021, 10, 278-283.	2.3	17
45	A New Twist on Scanning Thermal Microscopy. Nano Letters, 2012, 12, 1218-1223.	4.5	16
46	Giant surfactants for the construction of automatic liquid crystal alignment layers. Journal of Materials Chemistry C, 2019, 7, 8500-8514.	2.7	16
47	Reconfigurable Reflective Colors in Holographically Patterned Liquid Crystal Gels. ACS Photonics, 2020, 7, 1978-1982.	3.2	15
48	Electro- and Photo-Driven Orthogonal Switching of a Helical Superstructure Enabled by an Axially Chiral Molecular Switch. ACS Applied Materials & Interfaces, 2020, 12, 55215-55222.	4.0	14
49	Optimization of acoustically-driven ferromagnetic resonance devices. Journal of Applied Physics, 2019, 126, .	1.1	13
50	The contribution of chirality and crosslinker concentration to reflection wavelength tuning in structurally chiral nematic gels. Journal of Materials Chemistry C, 2014, 2, 132-138.	2.7	9
51	A Different Perspective on Cholesteric Liquid Crystals Reveals Unique Color and Polarization Changes. ACS Applied Materials & amp; Interfaces, 2020, 12, 37400-37408.	4.0	9
52	Topological Antiferromagnetic Van der Waals Phase in Topological Insulator/Ferromagnet Heterostructures Synthesized by a CMOS ompatible Sputtering Technique. Advanced Materials, 2022, 34, e2108790.	11.1	9
53	Size, weight, and power breakthrough in nonmechanical beam and line-of-sight steering with geo-phase optics. Applied Optics, 2021, 60, G154.	0.9	8
54	Responsive plasma polymerized ultrathin nanocomposite films. Polymer, 2012, 53, 4686-4693.	1.8	7

## MICHAEL E MCCONNEY

#	Article	IF	CITATIONS
55	Cycloidal diffractive waveplates fabricated using a high-power diode-pumped solid-state laser operating at 532Ânm. Journal of the Optical Society of America B: Optical Physics, 2019, 36, D136.	0.9	6
56	Temperature dependent resonant microwave absorption in perpendicular magnetic anisotropy epitaxial films of a spinel ferrite. Journal of Applied Physics, 2019, 125, .	1.1	5
57	Parallel pumping of spin waves in a ferromagnet revisited. Journal of Magnetism and Magnetic Materials, 2019, 490, 165486.	1.0	5
58	Switchable, broadband, polarization-independent diffractive optical components and systems. , 2018, , .		3
59	Electrically switchable large, thin, and fast optics. , 2018, , .		3
60	Nanoelectronics: Amorphous Boron Nitride: A Universal, Ultrathin Dielectric For 2D Nanoelectronics (Adv. Funct. Mater. 16/2016). Advanced Functional Materials, 2016, 26, 2771-2771.	7.8	2
61	Liquid Crystals: Thermally Induced, Multicolored Hyper-Reflective Cholesteric Liquid Crystals (Adv.) Tj ETQq1 1 0.7	784314 rg 11.1	BT_/Overloc
62	Homoepitaxial Mn3Ge films on ultra-thin Fe seed layer with high perpendicular magnetic anisotropy. Journal of Magnetism and Magnetic Materials, 2020, 514, 167146.	1.0	0
63	Director grating and two-beam energy exchange in a hybrid photorefractive cholesteric cell with a helicoidal polymer network. Journal of Applied Physics, 2020, 127, 125502.	1.1	0